

Support Information

Achieving 10.5% Efficiency for Inverted Polymer Solar Cells by modifying ZnO Cathode Interlayer with Phenols

Ping Fu^a, Xin Guo^a, Bin Zhang^b, Tao Chen^a, Wei Qin^a, Yun Ye^a, Jianhui Hou^b, Jian Zhang^c, Can Li^{a*}

^a*State Key Laboratory of Catalysis, Dalian Institute of Chemical Physics, Chinese Academy of Sciences, Dalian National Laboratory for Clean Energy, iChEM, 457 Zhongshan Road, Dalian 116023, China, The University of Chinese Academy of Sciences*

^b*State Key Laboratory of Polymer Physics and Chemistry Beijing National Laboratory for Molecular Sciences Institute of Chemistry, Chinese Academy of Sciences Beijing 100190, P. R. China*

^c*Guilin university of electronic technology, material science and engineering, 1 Jinji Road, Guilin 541004*

Ping Fu and Xin Guo contributed equally to this work.

*Corresponding author:

Prof. Can Li: canli@dicp.ac.cn

Phone: (86)-411-84379070

Materials: The donor poly[4,8-bis(5-(2-ethylhexyl)thiophen-2-yl)benzo[1,2-b:4,5-b']dithiophene-co-fluorothieno[3,4-b]thiophene-2-carboxylate] (PTB7-Th) and the acceptor fullerene derivative, [6,6]-phenyl-C₇₁-butyric acid methyl ester (PC₇₁BM) were purchased from 1-Material, Inc. MeOH, diethyl ether, 2-naphthol, chlorobenzene (99%), 1,8-diiodooctane (98%) and zinc acetate were purchased from Sigma-Aldrich Inc. The ethanolamine was purchased from Guangzhou Chemical Reagent Factory. All materials were used as received.

General methods: The ultraviolet–visible absorption spectra (UV-Vis) and optical transmittance spectra were measured on a Varian Cary 5500 spectrometer. Atomic force microscopy (AFM) height images were obtained using a Bruker Metrology Nanoscope III-D atomic force microscope in tapping mode under atmospheric conditions. The work functions of ZnO and ZnO/alcohols were measured in air by scanning Kelvin probe microscopy (SKPM) with a Bruker Metrology Nanoscope III-D atomic force microscope. Conducting AFM tips (SCM-PIT/PtIr, Bruker, USA) were used for this study with a typical spring constant of 2.8 N m^{-1} and a resonance frequency of 75 kHz. Typical scan line frequency was 0.3 Hz and each image contained 512×512 pixels. The surface potential images were unprocessed original data. Advancing contact angle measurements were performed using a DSA100 system (KRüSS). All infrared spectra were collected with a resolution of 4 cm^{-1} and 32 scans by a in-situ Fourier transform infrared spectrometer (Nicolet NEXUS 470) with an MCT detector. All of the spectra shown here are in the absorbance mode. The operating conditions of in-situ FT-IR were the following: The samples of ZnO were pressed into self-supporting wafers (ca. 25 mg) and mounted inside an IR cell. The ZnO films was used as the background. Then methanol gas was continuously bubbled into until the infrared spectra were no longer changing, record the IR. Finally elevated the situ pool at temperature of 373K for 10min, then cool down to room temperature, record the IR. Since 2-naphthol is solidified at room temperature, we conduct an experiment by a blending 2-naphthol into ZnO precursor solution. The operating conditions were the following: the blend solution was heated to 200 degrees for 10min, then repeated washing by ether dissolved 2-naphthol, centrifugal process, finally dried and infrared testing. The steady-state photoluminescence spectra were recorded on an FLS920 fluorescence spectrometer (Edinburgh Instruments) in air at room temperature.

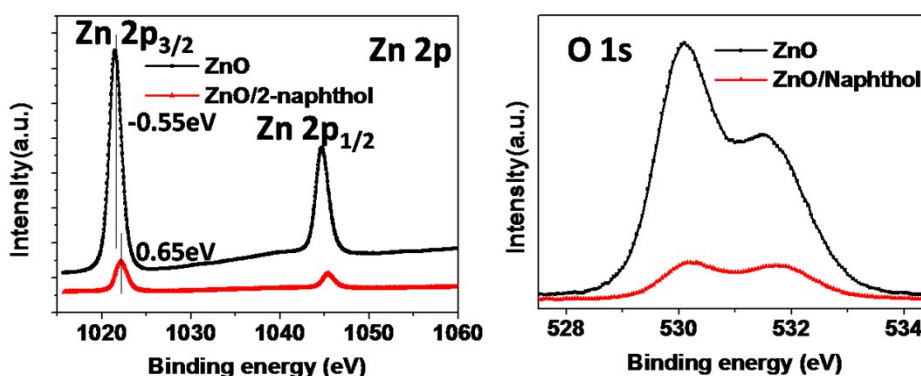


Figure.S1. X-ray photoelectron spectroscopy (XPS) (the Zn 2p and O1s peaks) of the ZnO and ZnO/2-naphthol film

In order to examine electron injection/transport capability of ZnO and naphthol modified ZnO films, Figure.S2(a) shows diode structures composed of a 100 nm-thick layer of PC₇₁BM sandwiched between ITO/CILs with a top Ca/Al electrode. Figure. S2(b) illustrates a comparison of the J-V characteristics of devices with ITO, ITO/ZnO, ITO/ZnO/MeOH or ITO/ZnO/2-naphthol. The voltage ($V > 0$) was applied to the top Al contact, electrons injected from CILs to PC₇₁BM and extracted from PC₇₁BM to Ca/Al. Devices with ITO required a larger applied bias for electron injection from ITO to PC₇₁BM because of the higher energy barrier. When the CILs were coated on ITO electrode, the required applied bias for electron injection/extraction was reduced, especially ZnO/2-naphthol as CIL, the required applied bias was the lowest. These differences are associated with the corresponding energy barrier height between CILs and PC₇₁BM.

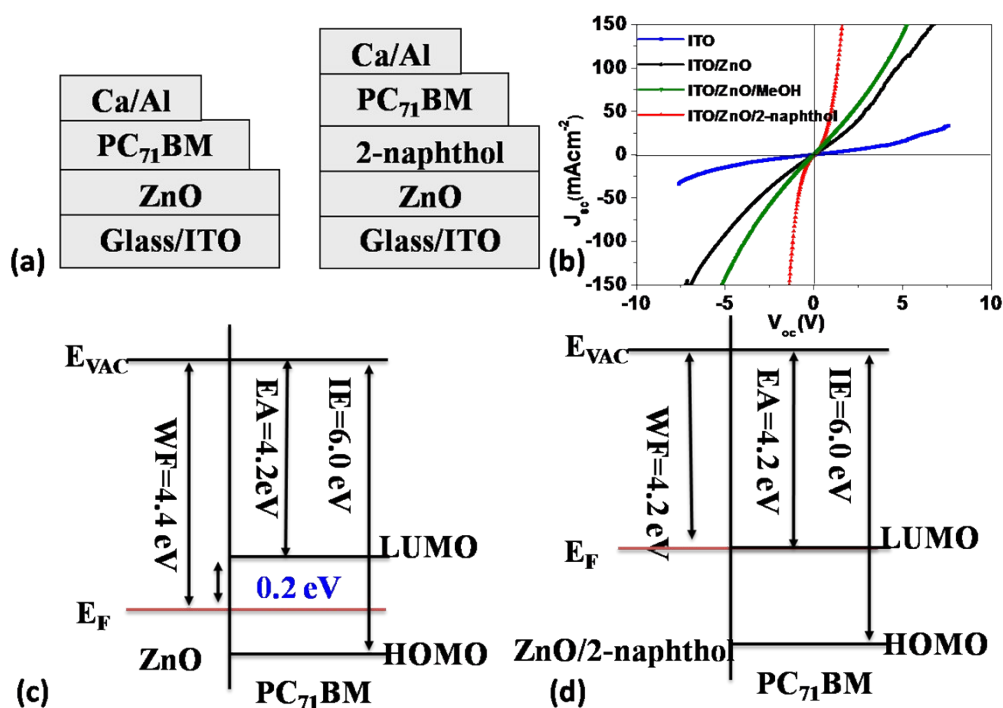


Figure S2. (a) Structure of devices with ITO/ZnO, ITO/ZnO/2-naphthol as the electrode.(b) The J-V characteristics of these devices. Energy level alignment of PC₇₁BM (100nm) on top of (c) ITO/ZnO and(d) ITO/ZnO/2-naphthol.

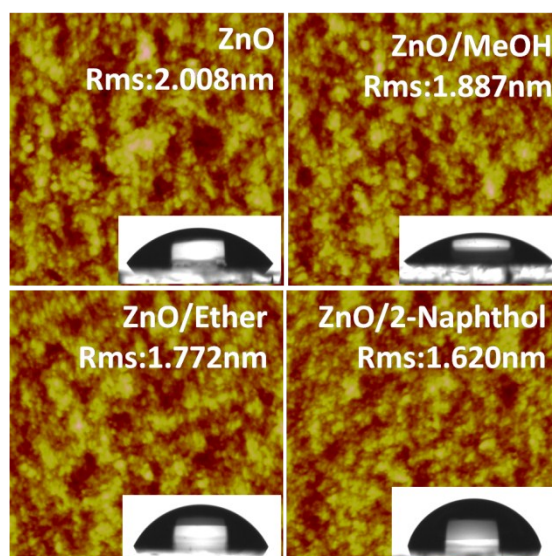


Figure S3. AFM topography images of the ZnO/BHJ films, ZnO/MeOH/BHJ films, ZnO/ether/BHJ films, and ZnO/2-naphthol/BHJ films. Photographs of water droplets on the surface of ITO substrates coated with ZnO, ZnO/MeOH, ZnO/ether and ZnO/2-naphthol in the illustration.

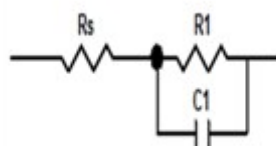


Figure S4. The equivalent circuit model for IPSCs in electrochemical impedance spectra.

Table S1. Summarized parameters of the IPSCs equivalent circuit with ZnO or ZnO/2-naphthol CILs measured at open voltage.

Element	ZnO	ZnO/2-naphthol
R_s (Ω)	36.44	25.07
R_1 (Ω)	706.4	422.8
C_1 (F)	3.32×10^{-9}	3.30×10^{-9}

Electrical impedance spectroscopy (EIS) measurement is conducted to analysis the conjugated polymer and interface properties of the PTB7-Th:PC₇₁BM IPSCs with ZnO or ZnO/2-naphthol CILs. Nyquist plots of devices were measured at open-circuit voltage based on ZnO and ZnO/2-naphthol. The fitted equivalent circuit model composed of series resistance (R_s) and component R_1 forming a parallel circuit with capacitor C_1 . The parameters of the IPSCs equivalent circuit with ZnO or ZnO/2-

naphthol CILs are summarized in Table S1. The (R_1, C_1) components are primarily affect by the CILs. The Nyquist plots that follow shows the R_s and R_1 of the devices with ZnO CILs are 36.44 Ω and 706.4 Ω , respectively, while the devices based on ZnO/2-naphthol, the R_s and R_1 suddenly decreases to 25.07 Ω and 422.8 Ω , respectively. The extracted contact resistance is notable reduced when the devices with ZnO/2-naphthol CILs.

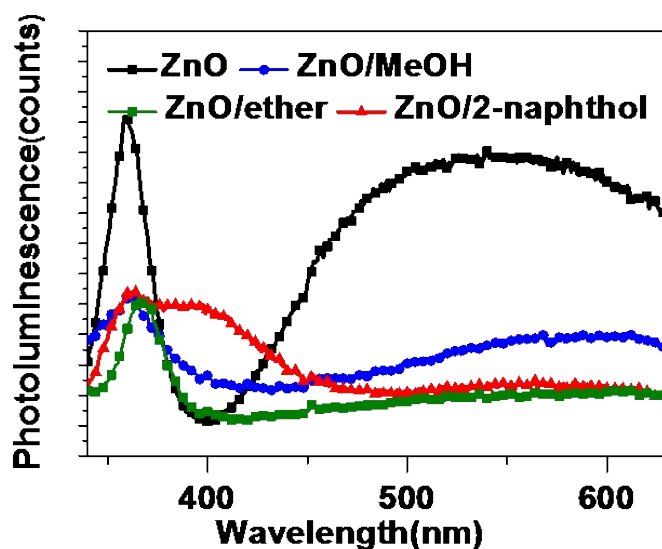


Figure S5. Steady-state fluorescence of the ZnO and modified ZnO films.

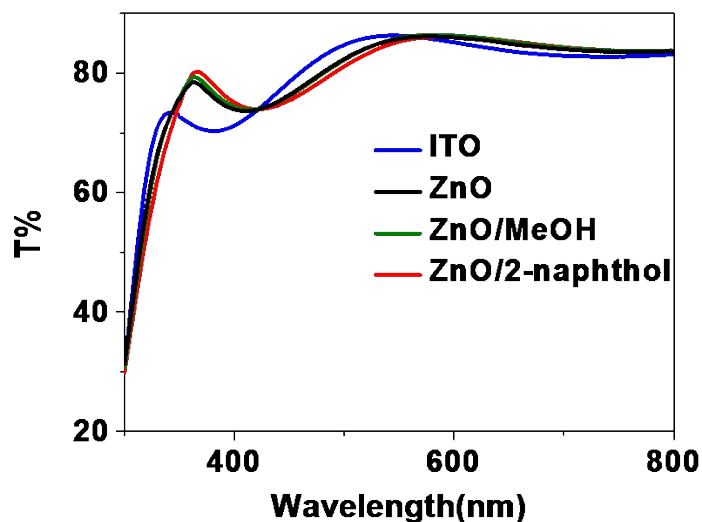


Figure S6. Transmission spectra of ZnO and modified ZnO films.

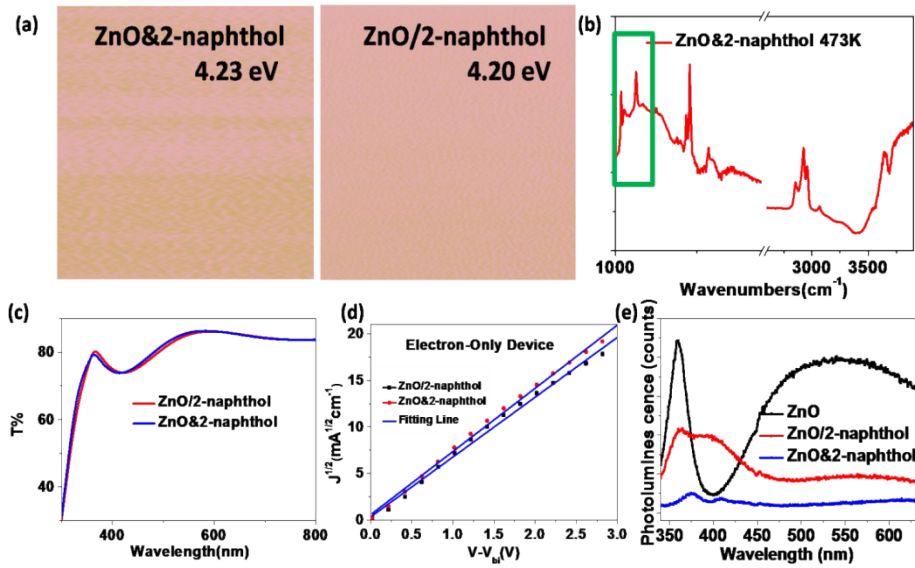
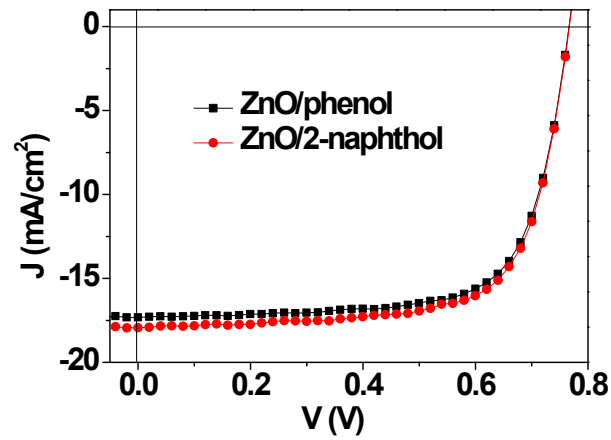


Figure S7.(a) WF of the ZnO&2-naphthol film and ZnO/2-naphthol film. (b) in-situ fourier transform infrared spectroscopy (FT-IR) of the mixture of ZnO and naphthol (ZnO&2-naphthol). The ZnO film was used as the background. (c)Transmission spectra, (d) Electron mobility, and (e) photoluminescence of the ZnO&2-naphthol film and ZnO/2-naphthol film.



CIL	J_{sc} (mA cm ⁻²)	V_{oc} (V)	FF(%)	PCE(%)
ZnO/phenol	17.37	0.76	72	9.50
ZnO/2-naphthol	18.01	0.76	72	9.79

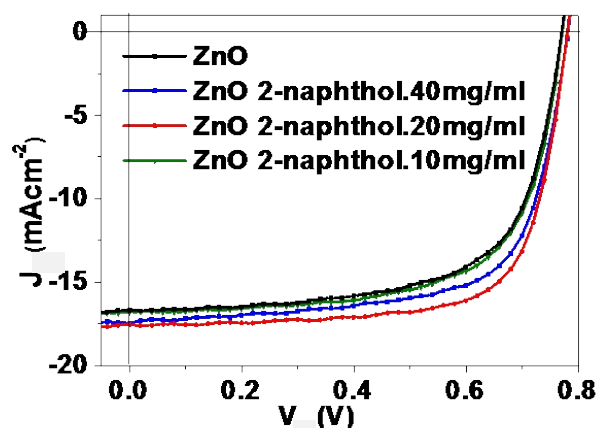


Figure S9. J-V curves of devices with different amount of 2-naphthol blending into ZnO film as CIL.

Table S3. The summary of device parameters of the IPSCs with different amount of 2-naphthol blending into ZnO film as CIL.

CIL	J_{sc} (mA cm ⁻²)	V_{oc} (V)	FF	PCE (%)
ZnO&2-naphthol 10mg/ml	17.43	0.78	0.68	9.30
ZnO&2-naphthol 20mg/ml	17.54	0.78	0.72	9.89
ZnO&2-naphthol 40mg/ml	16.81	0.76	0.68	8.68

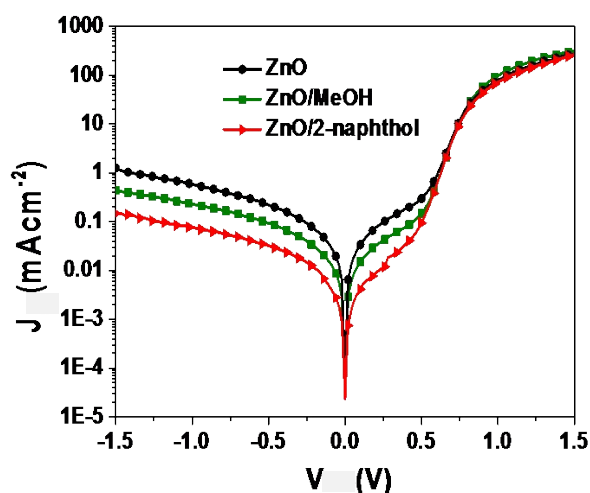


Figure S10. The dark J-V curves of the IPSCs with.

The reverse saturation current for the IPSCs with ZnO/2-naphthol CILs is greatly suppressed compared to the device with ZnO CIL, while they exhibit similar output current in the forward direction, improving the selectivity of the cathodes and giving a higher rectification ratio than that of IPSCs with ZnO. What's more, the lower

leakage current indicates the suppression of the bimolecular recombination by the IPSCs with combined ZnO/2-naphthol CILs. Thus, the combined results can be further explained the increase of J_{sc} and FF.

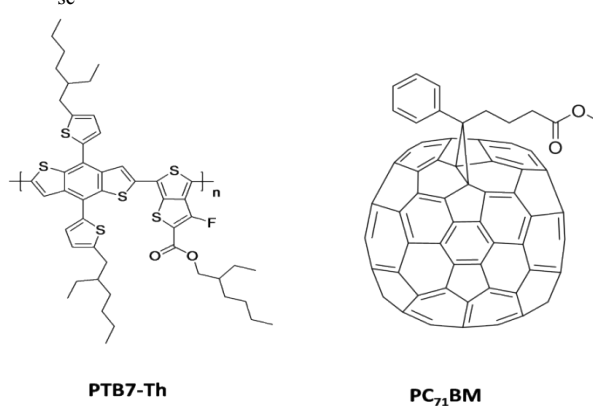


Figure S11. Chemical structures of PTB7-Th and PC₇₁BM used as donor and acceptor.

References:

1. F. X. Xie, W. C. H. Choy, W. E. I. Sha, D. Zhang, S. Q. Zhang, X. C. Li, C. W. Leung, J. H. Hou, *Energy Environ. Sci.*, 2013, **6**, 3372.
2. N. Baram, Y. Ein-Eli, *J. Phys. Chem. C*, 2010, **114**, 9781-9786.
3. F. Fabregat-Santiago, G. Garcia-Belmonte, I. Mora-Sero, J. Bisquert, *Phys. Chem. Chem. Phys.*, 2011, **13**, 9083.